

1 Using single remote sensing image to calculate the height of the  
2 landslide dam and the maximum volume of the lake

3

4 Weijie Zou <sup>1,2</sup>, Yi Zhou <sup>1</sup>, Shixin Wang <sup>1</sup>, Futao Wang <sup>1</sup>, Litao Wang <sup>1</sup>, Qing  
5 Zhao <sup>1</sup>, Wenliang Liu <sup>1</sup>, Jinfeng Zhu <sup>1</sup>, Yibing Xiong <sup>1,2</sup>, Zhenqing Wang <sup>1,2</sup>,  
6 Gang Qin <sup>1,2</sup>

7 <sup>1</sup>*Aerospace Information Research Institute, Chinese Academy of Sciences, Beijing, 100094, China;*

8 <sup>2</sup>*University of Chinese Academy of Sciences, Beijing 100049, China;*

9 *Correspondence: Yi Zhou (zhouyi@radi.ac.cn) and Futao Wang (wangft@aircas.ac.cn)*

10 **1. Abstract**

11 Landslide dams are caused by landslide materials blocking rivers. After the occurrence of large-scale  
12 landslides, it is necessary to conduct large-scale investigation of barrier lakes and rapid risk assessment.  
13 Remote sensing is an important means to achieve this goal. However, at present remote sensing is only  
14 used for monitoring and extraction of hydrological parameters at present, without prediction on potential  
15 hazard of the landslide dam. The key parameters of the barrier dam, such as the dam height and the  
16 maximum volume, still need to be obtained based on field investigation, which is time-consuming. Our  
17 research proposes a procedure that is able to calculate the height of the landslide dam and the maximum  
18 volume of the barrier lake, using single remote sensing image and pre-landslide DEM. The procedure  
19 includes four modules: (a) determining the elevation of the lake level, (b) determining the elevation of  
20 the bottom of the dam, (c) calculating the highest height of the dam, (d) predicting the lowest crest height  
21 of the dam and the maximum volume. Finally, the sensitivity analysis of the parameters during the  
22 procedure and the analysis of the influence of different resolution images is carried out. This procedure  
23 is mainly demonstrated through Baige Landslide Dam in south-west China. The single image from  
24 Beijing-1 and pre-landslide DEM, SRTM V3, are used to predict the height of the dam and the key  
25 parameters of the dam break, which are in good agreement with the measured data. And Hongshiyuan  
26 landslide dam is also used to validate the procedure. This procedure can effectively support the quick  
27 decision-making regarding hazard mitigation.

28

29 Keywords: Landslide dam, Remote sensing, DEM, Dam height, Hazard

## 2. Introduction

Landslide dams are caused by landslide materials blocking rivers, usually in mountainous areas with rivers and narrow valleys, bringing great risks to local people's lives and property(Costa and Schuster, 1988; Fan et al., 2020). Landslide dams disaster is widely distributed around the world. For instance, the 11 dams caused by the Magnitude 7.6 earthquake in New Zealand 1929(Adams, 1981); Oso Landslide Dam in Washington, USA in 2014(Iverson et al., 2015); Diexi Landslide Dam on Minjiang River, China, 1933(Li et al., 1986); Yigong Landslide Dam in 2000(Zhou et al., 2016) and a series of landslide dams including the Tangjiashan Landslide Dam caused by the Wenchuan earthquake in 2008(Zhang et al., 2019).-

Based on the historical records of 183 landslide dams, Costa found that the main way of dam breaching was overtopping. 41% of dams breached within one week, and 85% breached within a year(Costa and Schuster, 1988). Respectively Fan analyzed a series of dams induced by the 2008 Wenchuan earthquake finding that 43% of them collapsed within one month(Fan et al., 2012). And according to Shen's research on the longevity of the barrier lake, nearly 48.3% of the dams will breach within a week, and 84.4% of the dams will fail within one year(Shen et al., 2020). ~~Generally speaking, Most of~~ landslide dams are unstable. However, the landslide dam always occurred in remote mountainous areas, with inconvenient traffic conditions and poor infrastructure(Cui et al., 2009). When earthquakes or precipitation induce large-scale landslides, field survey is time-consuming and manpower-consuming(Dong et al., 2014). Remote areas tend to be more vulnerable and the dam breaching are more likely to cause serious consequences. So, it requires us to identify the landslide dam and take action as quickly as possible.

There are several factors influencing the process of formation, development and risk of landslide dams. These factors can be divided into three categories. First, the factor of the soil, including the dam material composition and the repose angle of the dam material, has an unavoidable relationship with the formation and erosion process of the dan. The low permeability and high erodibility will lead to short longevity of the landslide dam and fast breaching of the dam(Shen et al., 2020). Second, the hydrological parameters, such as lake volume, average annual discharge and catchment area which decide the speed of lake surface raising(Cao et al., 2011). The faster the lake raises, the less time is left to hazard mitigation. Third, the geometric parameters, such as the length and angle of the landslide surface and the length, width, height of the dam. The landslide surface influences the kinetic energy of the landslide material which has a great influence on the formation of the landslide dam. And the geometric parameters of the dam itself decide the stability of dam, the maximum volume of the lake and the potential maximum discharge of breaching (Dong et al., 2011a; Cao et al., 2011; Shen et al., 2020).

Remote sensing has the ability to identify and monitor landslide dams on a large scale conveniently, and ~~can~~ supports quick decision-making regarding hazard mitigation(Canuti et al., 2004; Fan et al., 2021). In the research before, remote sensing is usually regarded as an auxiliary means to monitor the change of

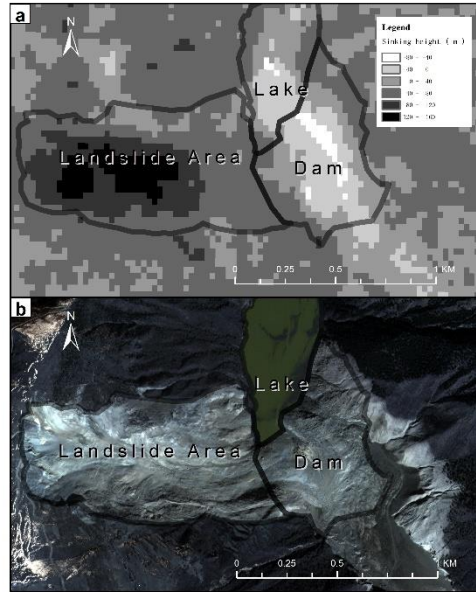
67 the catchment area or to measure the length of the dam. For example, Wang and Lv used multiple remote  
68 sensing images to extract water boundary images and pre-landslide DEM to monitor the changes of lake  
69 volume of Yigong Lake(Wang and Lu, 2002). Respectively, Cheng et al. proposed a method to estimate  
70 reservoir capacity of water based on water boundary and DEM(Chen and Lu, 2008).

71 The researches above focused on obtaining information of the barrier lake through remote sensing and  
72 Geographic Information System. However, these kinds of methods focus on monitoring and can only  
73 obtain part of geometry parameters directly through image such as catchment area, and lack judgment of  
74 future development of the landslide dam. Some essential components of hazard evaluation are not  
75 available in these researches. Especially the height of the dam which determines the maximum volume  
76 of the barrier lake and the flood peak of the dam breaching(Costa and Schuster, 1988; Ermini and Casagli,  
77 2003; Peng and Zhang, 2012; Dong et al., 2014) can't be obtained through these methods. However, as  
78 most of the landslide dams breach by overtop, they start to breach as long as the elevation of lake surface  
79 equals the elevation of the landslide dam(Meng et al., 2021; Costa and Schuster, 1988; Ermini and  
80 Casagli, 2003). So, the height of the landslide dam decides the maximum volume of berried lake. The  
81 damage of the landslide dam mostly relies on the flood it causes through breaching. As water goes  
82 through the dam surface, the erosion process will lead to rapid increase of the discharge and finally result  
83 in flood. According to research, his process has a strong relationship with the height of the landslide  
84 dam(Anon, 2021; Shen et al., 2020; Chen et al., 2004; Braun et al., 2018), which makes it one of the  
85 most important parameters related to this hazard. –

86 With the rapid development of Unmanned Aerial Vehicles (UAVs), in 2008, photogrammetric UAVS are  
87 also used to survey the landslide dams in the Wenchuan earthquake in 2008(Cui et al., 2009). However,  
88 after the earthquake, there are to be a large number of landslides and the affected area is considerably  
89 huge. If UAVs are used for precise investigation one by one, it cannot meet the requirements of timeliness  
90 for the emergency. Based on the pre-landslide DTM and a series of remote sensing images after the  
91 landslide dam, Dong obtains the variation of the lake level to estimate the slope foot of the barrier dam  
92 and predict the dam height, completing quickly assessment of the dam breaching hazard(Dong et al.,  
93 2014). But this procedure is still inconvenient as it requires sequential images to predict the height of the  
94 dam.

95 What's more, aAll of the methods that use the pre-landslide DEM are based on an important assumption  
96 that the pre-landslide DEM is reliable. Nevertheless, take Baige Landslide Dam as example (Fig 1), we  
97 can find that the elevation of landslide area changes greatly. The landslide area has a greater degree of  
98 subsidence, and the dam area has a greater degree of uplift. And even in areas nearby covered with  
99 vegetation, there was about 20 meters of subsidence averagely, which demonstrates that the assumption  
100 above nee further improvement.

101 This research will focus on the weakness above using single remote sensing image and pre-landslide  
102 DEM to obtain the essential information of the landslide dam and calculating the height of the landslide  
103 dam based on the formation mechanism of the landslide dam. The Baige Landslide Dam is taken as an  
104 example to verify the feasibility of this procedure. And the sensitivity analysis of the parameters during  
105 the procedure and the analysis of the influence of different image resolution will be carried out in the  
106 discussion part.

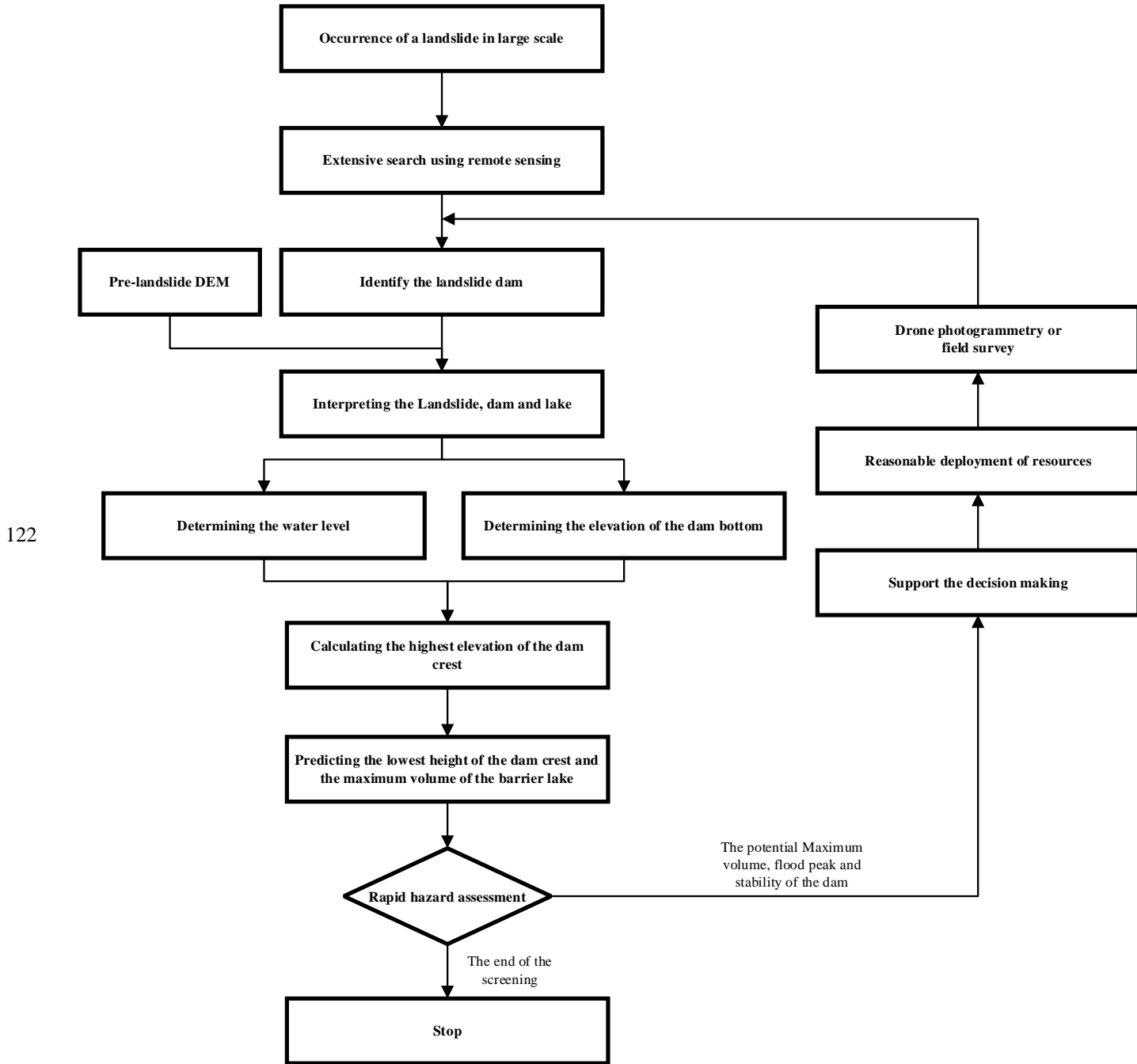


107

108 Fig 1 picture a is the comparison of pre-landslide DEM (SRTM V3) and the after-landslide ~~Dem~~DEM.  
 109 And picture b is the remote sensing image from Beijing-1 satellite (taken in November 9, 2018)

### 110 3. Procedure

111 After the occurrence of large-scale landslides, the government often can't get all the disaster situation  
 112 immediately, so large-scale landslides investigation is needed. As the disaster often occurs in remote  
 113 areas, the purpose of the large-scale investigation is not only to find the landslide dams, but also to make  
 114 an objective evaluation of the hazard of the landslide dams, supporting reasonable allocation of resources  
 115 to avoid excessive reaction. When a landslide dam is identified from the image, the procedure to calculate  
 116 its height is divided into four parts: (a) selecting the reference points to determine the elevation of the  
 117 lake level; (b) estimating the elevation of the bottom of the dam; (c) calculating the highest elevation of  
 118 the dam crest based on the formation mechanism of the landslide dam; (d) predicting the lowest height  
 119 of the dam crest and the maximum of the lake volume. This section will elaborate the details of (a), (b),  
 120 (c) and (d), obtaining the lowest height of the dam crest and calculating the maximum volume based on  
 121 GIS.



123  
124 Fig 2 the procedure of obtaining the height of the dam crest and completing the hazard assessment

125  
126 This study provides a method to predict critical information about a barrier dam using limited real-time  
127 data. The data required includes an after-landslide satellite image and a pre-event DEM. The data that  
128 is not required include the repose angle of the nearby material and the elevation of the riverbed. If there  
129 are reliable recordings, they can be used in the procedure to improve the prediction accuracy.  
130 Otherwise, our research provides a reliable method to predict them. The whole prediction of dam  
131 elevation information based on the above input data will be explained in the following sections. The  
132 process of use of each input data, determination of intermediate parameters and final output results is

shown in Fig 3.

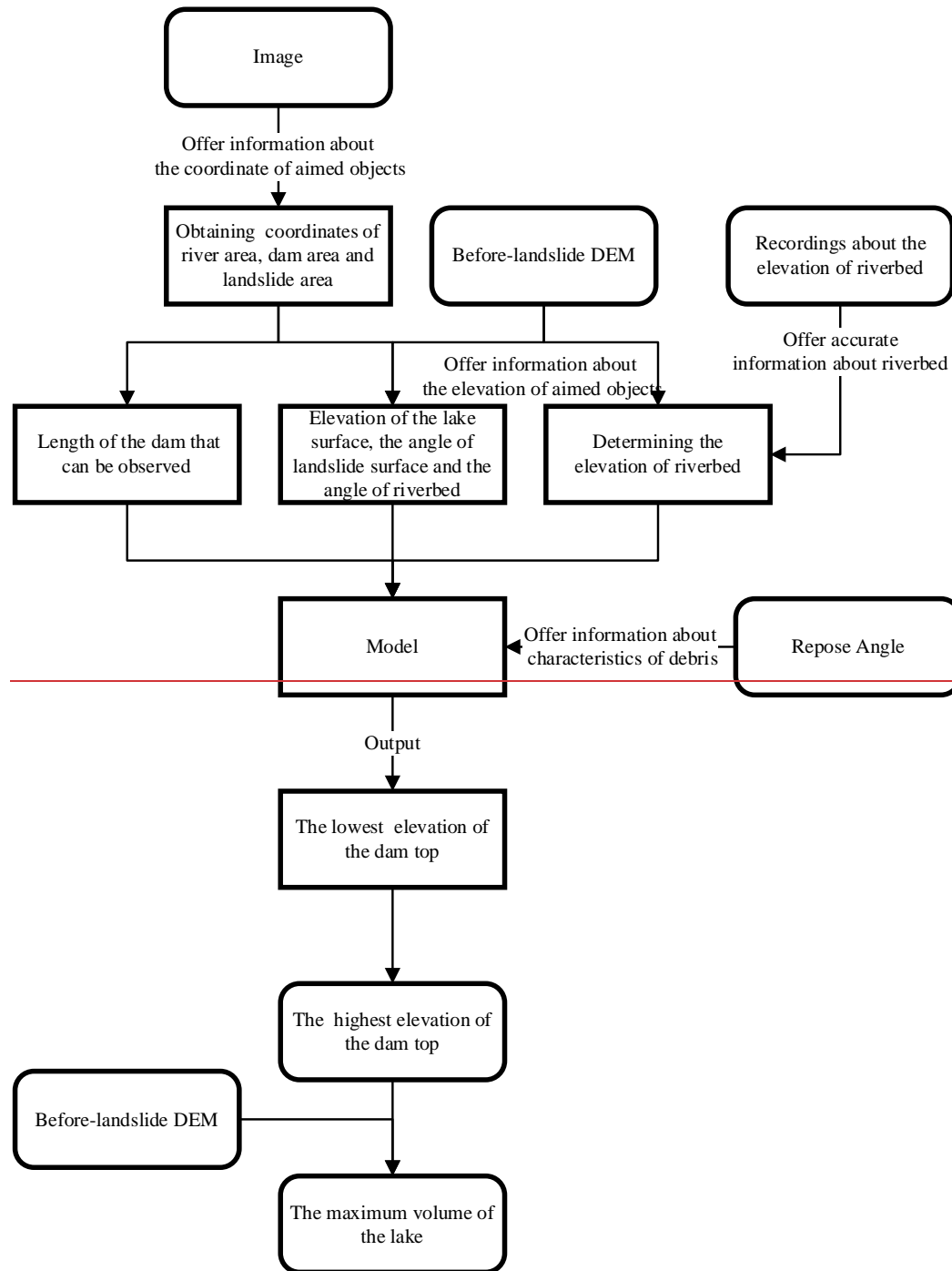


Fig 3 the complete process of determination of parameters in the procedure of prediction

### 136 3.1. Determining the elevation of the lake level

137 The method of estimating the elevation of the barrier lake based on remote sensing images has been  
138 practiced by many scholars. Typically speaking, researchers assume that the elevation of the water  
139 boundary is the same as the topography. And pre-landslide DEM is used in most cases to determine the  
140 lake level with the water boundary in the image(Wang and Lu, 2002; Chen and Lu, 2008; Dong et al.,  
141 2014; Braun et al., 2018). However, the reliability of the pre-landslide DEM may decrease as a result of  
142 landslides (Fig 1). The reasons are summarized as follows: (a) the landslide has caused some changes in  
143 the topography of the area; (b) the pre-landslide DEM has errors itself, especially in the mountainous  
144 area; (c) as the pre-landslide DEM usually can not be undated in time, there can be some landslides  
145 without records before.

146 For the reasons above, the selection of the reference points to determine the elevation of the lake level  
147 should follow these principles to reduce errors. (a) As landslides often bring about large-scale ground  
148 subsidence, when selecting reference points, the point around the landslide area should be avoided. (b)  
149 Because landslides and settlements tend to occur in areas with steep terrain and little vegetation  
150 coverage(Ayalew and Yamagishi, 2005) and the DEM is more precise in flat terrain, the reference points  
151 should be in vegetation-covered flat terrain, avoiding gully or ravines.

152 Under these strictions the reference points selected can be regarded as having the same elevation of the  
153 lake level. Therefore, the lake level is determined. However, in order to determine the elevation of the  
154 lake level, a complex number of reference points are needed. Their value can't be the same for the random  
155 errors but should be within a certain range(Fig 6), for the random errors of DEM and the errors in the  
156 process of determining the points. In this situation, points that are one and a half interquartile range away  
157 from the mean value are considered outliers. And the elevation of the lake level is the average elevation  
158 of the remains. Because the dam blocks the channel and the river has no outflow, the water surface can  
159 be assumed to be still(Wang and Lu, 2002; Morgenstern et al., 2021; Fan et al., 2021). So, the elevation  
160 of the lake level is the same as the elevation of the dam-lake point in Fig 3.

### 161 3.2. Determining the elevation of the dam bottom

162 In this procedure, the bottom of the dam refers to the point where the dam meets the river bed on the  
163 downstream side. In practical cases, the most reliable method is to directly use the riverbed elevation  
164 obtained recently. In the absence of relevant data, the following method should be taken for prediction.

165 Within a certain range, the riverbed elevation can be considered to decrease in proportion along the  
166 channel, conforming to a linear variation. Therefore, sampling elevation points at the lowest point of the  
167 river valley in the pre-landslide DEM, removing the outliers and carrying out simple regression to obtain  
168 the fitting of the riverbed elevation. By extending the fitting results to the dam body and subtracting the  
169 historical river depth, the bottom elevation of the dam is obtained.

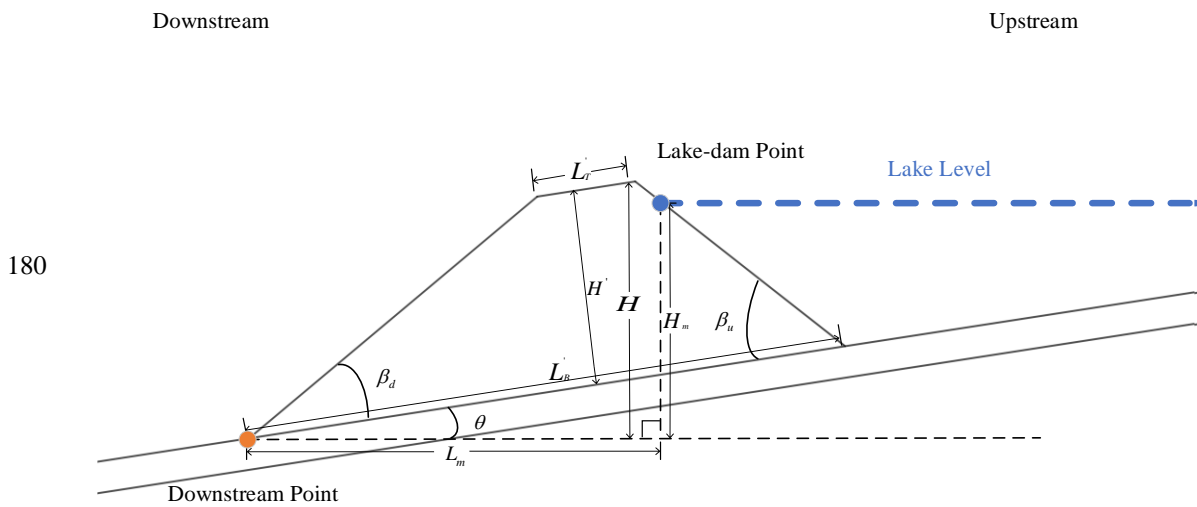
170 However, the historical river depth is to vary with the seasons. So, there must be some errors in this  
171 prediction. The influence of dam bottom elevation on calculating dam height will be analyzed in the

172 “discussion” section.

### 173 3.3. Calculating the highest elevation of the dam crest

174 According to Wu's laboratory experimental study, the geometrical form of the barrier dam is mainly  
 175 determined by landslide slope, river slope, angle of repose, earthwork amount and sliding height. I (Wu  
 176 et al., 2020).

177 With his theory, if the river is completely blocked and the valley can be simplified into U-shape, the  
 178 longitudinal section of the landslide dam can be simplified as a trapezoid(Wu et al., 2020) as shown in  
 179 Fig 4. And the trapezoid will follow the following pattern.



181 Fig 43 simplified section of the landslide dam

182 The top of the dam is parallel to the bottom of the dam (Wu et al., 2020).

183  $L_T \parallel L_B$  (1)

184 Where  $L_T$  is the top of the dam,  $L_B$  is the bottom of the dam (Wu et al., 2020).

185  $\beta_d + \theta = \beta_u - \theta = \chi\varphi$  (2)

186 Where  $\beta_d$  is the angle between the body of the dam and the riverbed on the downstream side,  $\beta_u$  is  
 187 the angle between the body of the dam and the riverbed on the upstream side,  $\varphi$  is the angle of repose  
 188 of the landslide mass and  $\chi$  is the parameter that fits the effect of “cut top” phenomenon.  $\varphi$  is  
 189 determined by the nature of the soil itself and  $\chi$  will be affected by landslide surface angle, landslide  
 190 length and other factors(Grasselli et al., 2000). The determining of the  $\chi$  can be simplified as  
 191 follows(Wu et al., 2020):

192  $\chi = 0.57 + 0.51(1 + e^{\frac{(\alpha-34)}{10.50}})^{-1}$  (3)

193 where  $\alpha$  is the angle of the landslide surface. As the angle is higher, the actual angle between the  
 194 riverbed and the landslide material will be smaller and the length of the dam along the river will be longer.  
 195 Normally speaking, this formula fits the actual situation well. The precise of this fitting will be discussed



196 in the “discussion” section.

197 According to Wang's field investigation on the Wenchuan earthquake, it is found that the angle of repose  
198 of landslide dam in the Wenchuan earthquake is between 28.8° and 44.7°, with an average of 35.5° (Wang  
199 et al., 2013). In the absence of relevant data, it is recommended to use the average provided by Wang.

$$200 \quad \varphi = 35.5^\circ \quad (4)$$

201 Wu proposed that the height of the dam has a certain relationship with the length of the bottom of the  
202 dam (Wu et al., 2020), as follows:

$$203 \quad H' = (0.37 + 1.1 \tan \theta) \cdot \tan(\beta_d + \theta) \cdot L'_B \quad (5)$$

204 where  $H'$  is the height between the dam top and the dam bottom,  $\theta$  is the angle of the riverbed and

205  $L'_B$  is the length of the dam along the river. The  $R^2$  of formula (1) (2) (3) (5) are all greater than 0.95.

206 As shown in Fig 3, the elevation of the dam-lake point and the elevation of the dam bottom has already

207 been obtained before. So,  $H_m$  can be calculated and  $L_m$  can be obtained directly from the remote

208 sensing images. According to formula (1), (2), (3), (4) and (5), using simple geometric relations, the

209 following relation can be obtained:

210

$$211 \quad L'_B = \frac{L_m}{\cos \theta} + \frac{\cos(\beta_u - \theta)}{\sin \beta_u} \cdot (H_m - L_m \cdot \tan \theta) \quad (6)$$

$$212 \quad \underline{H_r = \sin \theta \cdot (L'_B - H' \cdot \tan \theta - H' \cdot \tan(90 - \beta_u))} \quad (7)$$

213

$$214 \quad H = \frac{H'}{\cos \theta} + H_r \quad (87)$$

215 Where  $H$  is the difference between the highest elevation of the dam crest and the dam bottom elevation

216 and  $H_r$  is the difference of the elevation of the riverbed between the dam bottom and the crest.  $\theta$  and

217  $\alpha$  can be obtained through the remote sensing image and the pre-landslide DEM easily.

218 Through this procedure, the highest elevation of dam crest is determined based on a single image and

219 pre-landslide DEM, which can be used in the further prediction of the dam breaching and related

220 decision-making.

### 221 3.4. Predicting the lowest height of the dam crest and the

### 222 maximum volume of the barrier lake

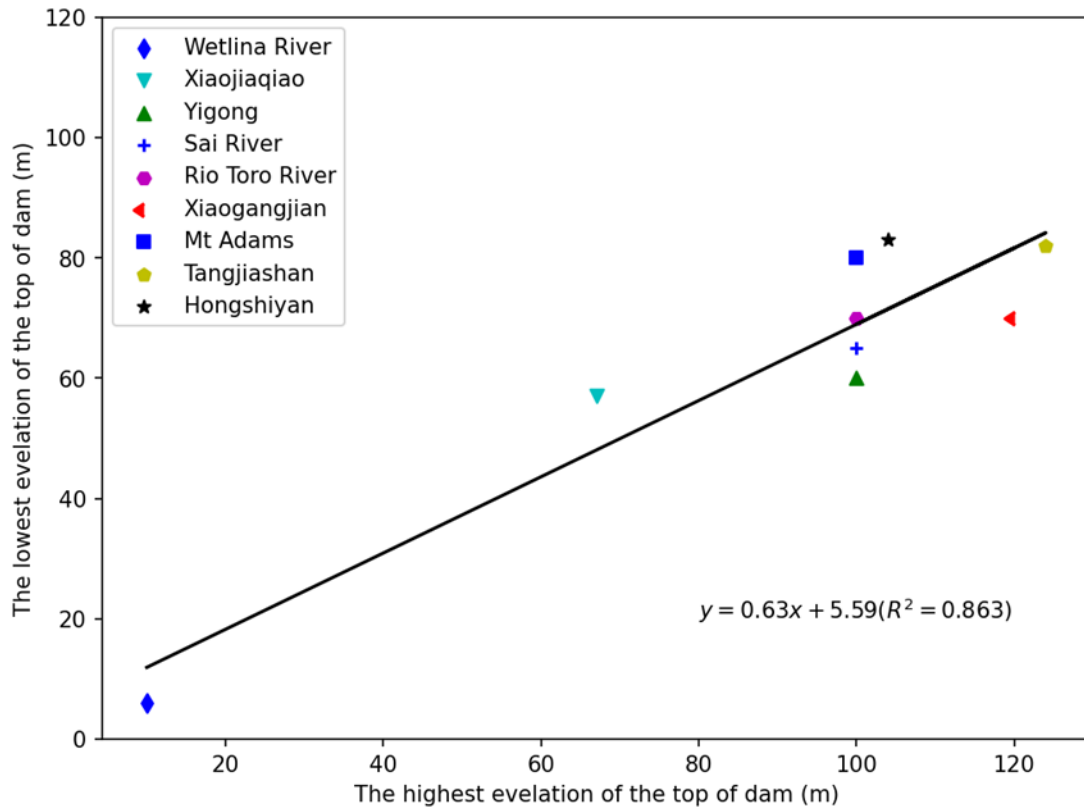
223 Because the height of the landslide dam in the vertical direction of the river channel will not be

224 consistent (Costa and Schuster, 1988; Fan et al., 2020), but will form different types of distribution

225 according to the characteristics of the case, resulting in the height of the landslide dam is not a simple

226 value but a range. As the most important factor affecting the dam break of a barrier lake dam breaching

227 is the height of the lowest point of the dam crest, which determines the potential maximum volume of  
 228 the barrier lake and the maximum discharge volume of the dam breach(Costa and Schuster, 1988; Chen  
 229 et al., 2004, 2021; Dong et al., 2011b, 2014; Yang et al., 2013; Zhong et al., 2018), the prediction result  
 230 of the highest elevation of the dam crest can't be used in related breaching models directly.  
 231 But by simply analyzing the highest elevation of the dam crest and the lowest elevation in the existing  
 232 records, a simple estimation of the relationship between them is carried out, as shown in Fig 54.



234 Fig 54 the relationship between the highest elevation of the dam crest and the lowest elevation of the  
 235 dam crest. These dataes ~~come from~~ can be found in the papers of Cui, Costa, Mora and so on(Costa and  
 236 Schuster, 1991; Mora Castro, 1993; Briaud, 2008; Cui et al., 2009; Peng and Zhang, 2012; Chen et al.,  
 237 2020).

238 .  
 239 The relationship can be expressed as follows:

240 
$$H_l = 0.63H_h + 5.59(R^2 = 0.863) \quad (98)$$

241 where  $H_l$  is the lowest elevation of the dam crest and  $H_h$  is the highest elevation of the dam crest.

242 On the basis of the formula above, we can use this procedure to complete the rapid assessment of the  
 243 breaching hazard.

244

245

## 4. Validation of the proposed procedure

246

### 4.1. Baige Landslide Dam

247

The Jinsha River, the upper reach of the Yangtze River, was dammed twice recently at Baige, Tibet, one

248

on 10 October 2018 and the other on 3 November 2018 (UTC+8), at  $98^{\circ}42'32.24''\text{E}$ ,  $31^{\circ}4'59.27''\text{N}$ (Fig

249

4) (Zhang et al., 2019) and one on November 3, 2018, the residual landslide of "10.10" Baige Landslide

250

Dam slid down again, forming "11.03" Baige Landslide Dam on the basis of the original residual dam(Li

251

et al., 2019). The dam is much larger than the first one, as the width of the dam top is 195 m, the length

252

of the dam top is 273 m and the highest elevation of the dam crest is 3014m(Chen et al., 2020). After

253

proper treatment, its storage capacity is reduced from  $8.69 \times 10^8 m^3$  to  $5.79 \times 10^8 m^3$  and the flood

254

peak is diminished from  $41624 m^3 / s$  to  $31000 m^3 / s$  (Chen et al., 2020; Yunjian et al., 2021). A

255

large number of roads and bridges were damaged downstream, and a total of 54,000 people were affected,

256

with economic loss of over 7.43 billion yuan(Zhang et al., 2019). Due to abundant field survey data and

257

its great harm, Baige Landslide Dam was selected to demonstrate this procedure.

258

Baige Landslide Dam occurred in a deep valley of the mountainous area and the barrier lake is long and

259

narrow (Fig ~~6~~5). To demonstrate the proposed procedure, we take the second Baige landslide as example.

260

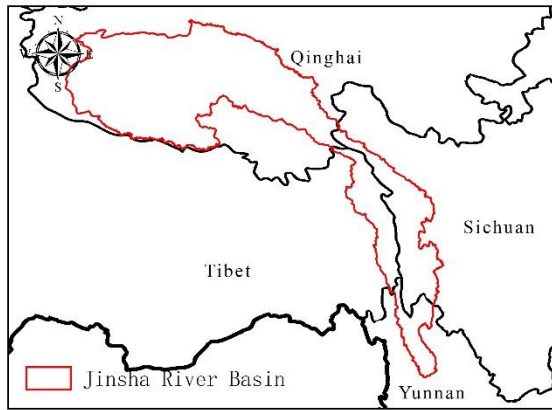
The image used is a 0.8m resolution image from Beijing-1 which was taken on November 9, 2018 and

261

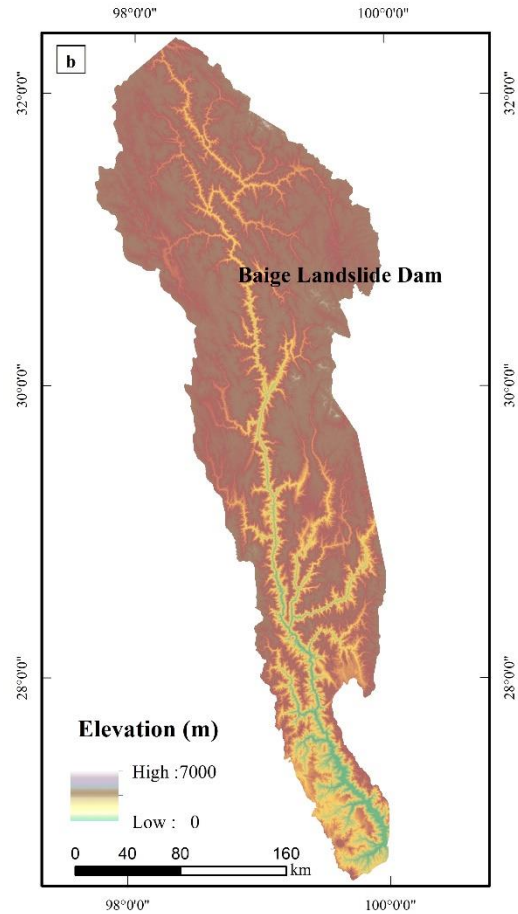
the pre-landslide DEM we choose is SRTM V3 of 30m resolution which was taken in 2000. The effect

262

of the resolution of the image will be discussed in the "Discussion" section.



263



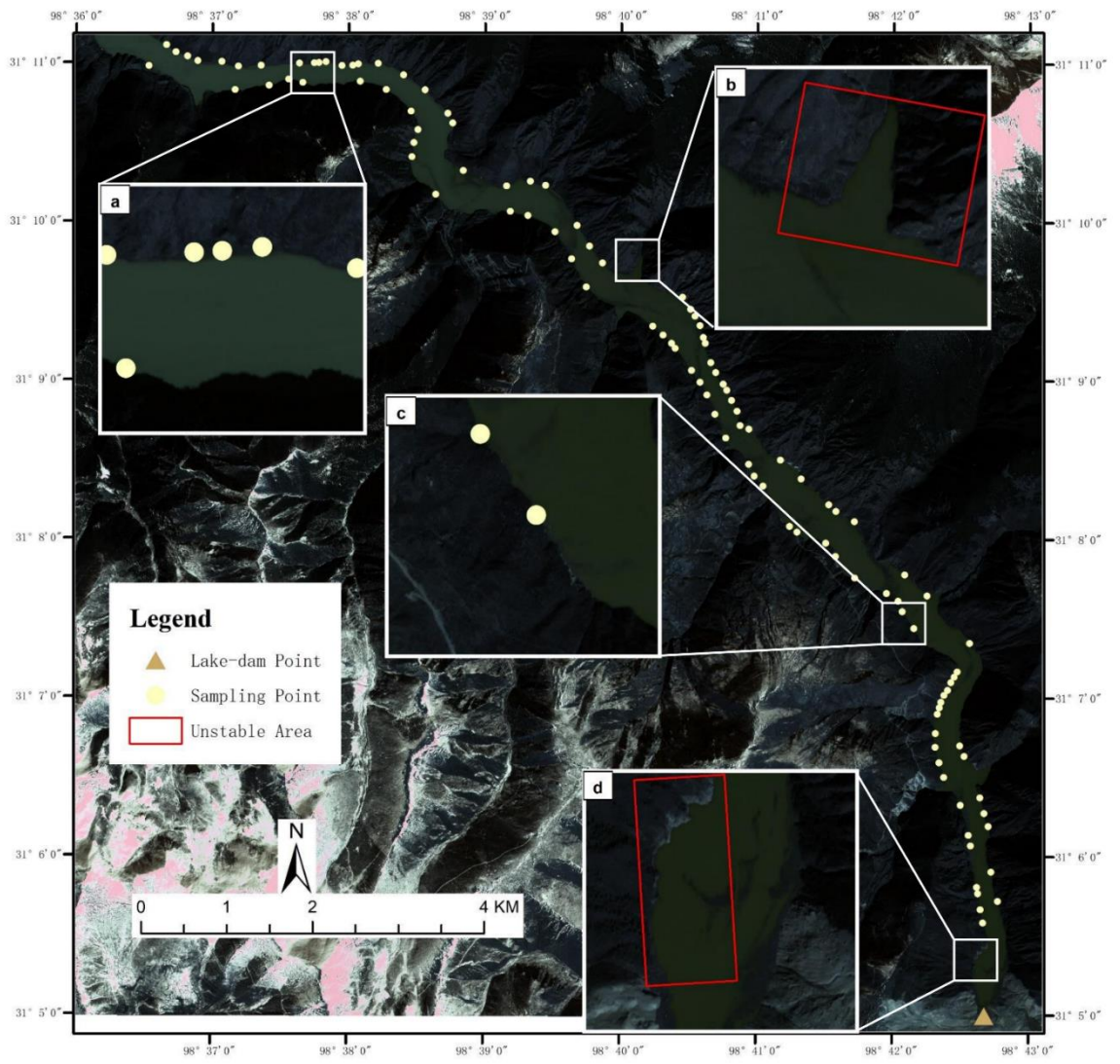
264 Fig 65 the position of the Baige Landslide Dam

265 4.2. Determine the elevation of the lake level

266 At the water boundary in the remote sensing image, the area covered by vegetation with relatively flat  
 267 terrain and a certain distance from the landslide was selected for elevation sampling (Fig 6). Under ideal  
 268 circumstances, the distribution of sampling points' elevation should be completely consistent. But in  
 269 practice, there are often large deviations, shown in Fig 87, the specific reasons for which have been  
 270 discussed in the "Procedure" section and will not be repeated. The deviation between the maximum and  
 271 minimum elevation of sampling points can reach 72m, and the shape basically conforms to the normal  
 272 distribution. Therefore, the mean of reference points can be obtained directly after clearing the outliers,  
 273 which is the elevation of barrier lake and the outcome is 2944m. Since the lake is essentially still, the  
 274 elevation of the lake should be the same as the elevation of the point where the dam meets the lake,  
 275 shown as the triangle in Fig 76.

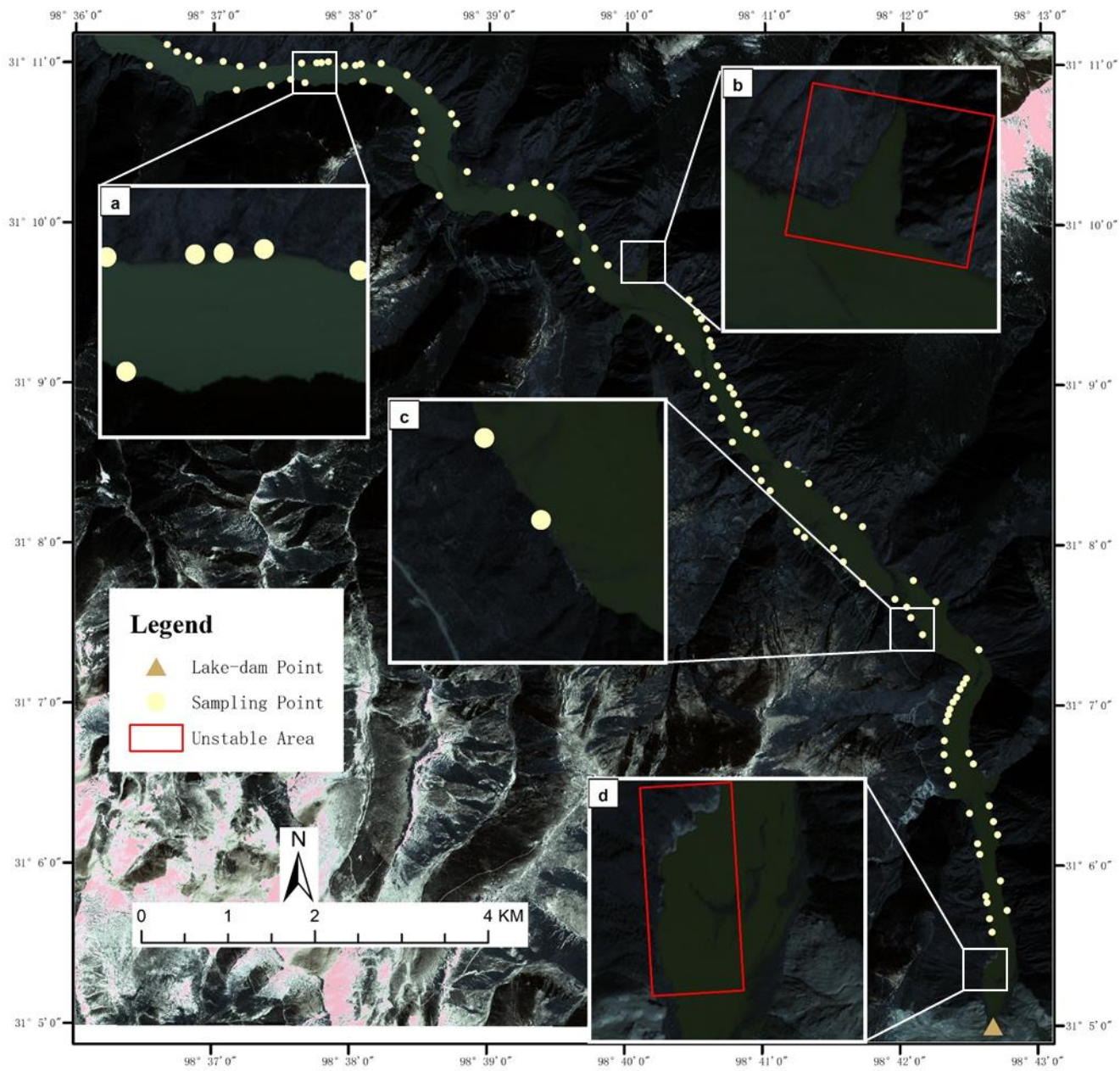
276

277



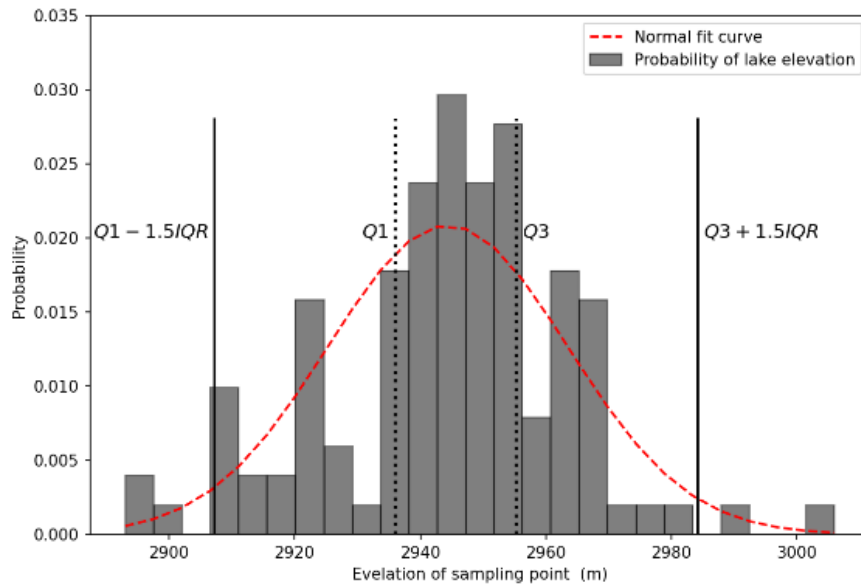
278

279



280 Fig 76 the sampling points in the case of Baige Landslide Dam (image from Beijing-1 satellite)

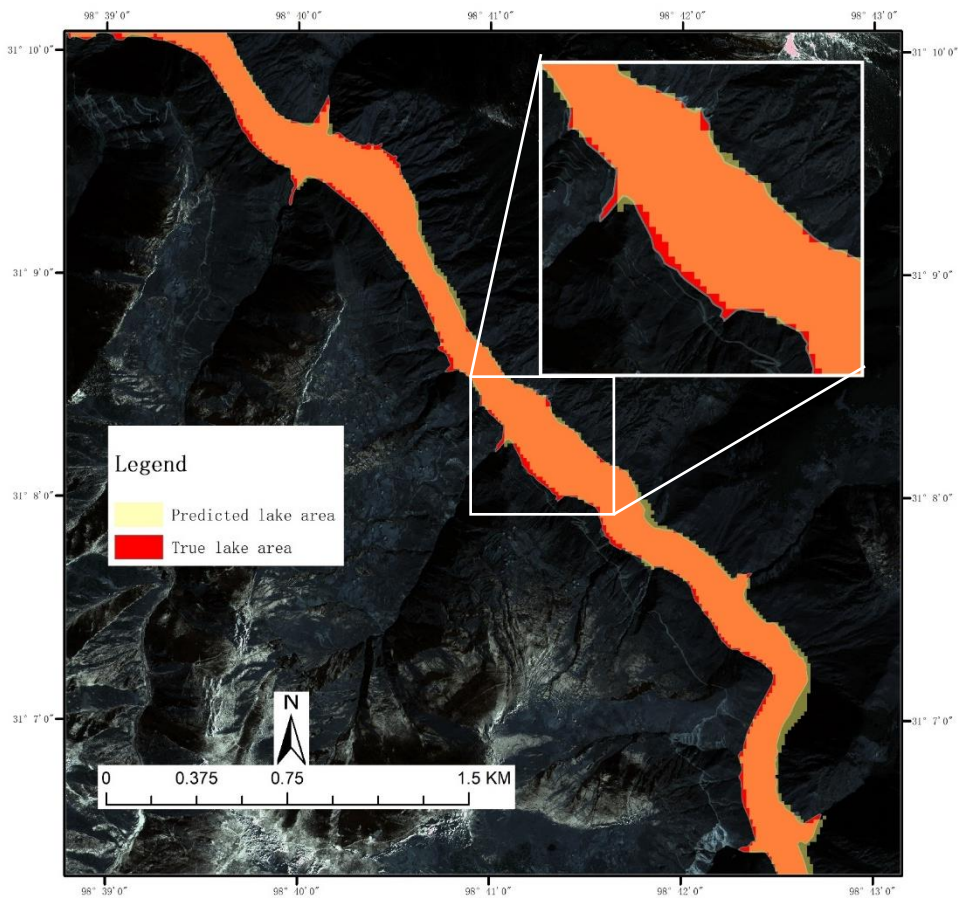
281



282 Fig 87 elevation distribution of sampling points

283 The Intersection over Union (IOU) of the area with elevation below 2944m in DEM and the actual  
284 submerged area in the remote sensing image is 84.48% (Fig 98). The two are found to be basically  
285 consistent.

286



287 Fig 98 the comparison of the area with elevation below 2944m in DEM and the actual submerged area

288 in the remote sensing image (image from Beijing-1 satellite)

289

290

291

### 292 4.3. Determining the elevation of the dam bottom

293 The inclination angle of the riverbed is calculated by sampling and unitary regression and is about  $0.11^\circ$ .

294 The elevation of the water level on the place of dam bottom before the landslide is 2867m. As the water  
295 depth is not considered when obtaining DEM and varies with change of rainfall in the rainy season and  
296 dry season, this value can't be used directly. According to the data in China Ministry of Water Resources  
297 Information Center, the water depth of Jinsha River section is about 2-10m. The water depth can be  
298 assumed as the mean value, 6m. Therefore, the final estimate of the dam bottom elevation is 2861m.  
299 Respectively, according to the field survey, the riverbed elevation is 2860m(Chen et al., 2020).

300

### 301 4.4. Calculating the highest height of the dam crest

302 The slope angle of the landslide surface, the inclination angle of the riverbed and the length of the  
303 landslide can be calculated directly through remote sensing image and DEM. The slope angle of landslide  
304 surface is  $30.65^\circ$ . The inclination angle of the riverbed is  $0.11^\circ$ . And the length of the landslide that can  
305 be observed is 567m. According to formula (5) (6) (7) (8), with the parameters obtained before, the  
306 highest height of the dam top is 155.4m and the highest elevation of the dam top is 3016.5m with an error  
307 of 2.5m compared to the measured data by Chen, 3014m(Chen et al., 2020).

### 308 4.5. Predicting the lowest height of the dam crest and the

#### 309 maximum volume of the barrier lake

310 Taking Baige Landslide Dam as an example, according to the case section, we have predicted that the  
311 highest elevation of the dam crest is 3016.5m and the height of the dam is 155.4m. According to formula  
312 (9), we calculated that the lowest height of the crest of the landslide dam is 104.2m, and the elevation  
313 is 2964.2m with an error of 2.8m compared to the measured data by Chen, 2067m(Chen et al., 2020).

314 Using Geographic Information System, we can estimate based on DEM(Wang and Lu, 2002; Chen and

315 Lu, 2008) that its potential maximum volume is  $7.96 \times 10^8 (m^3)$ .



## 4.6. Another case for validation

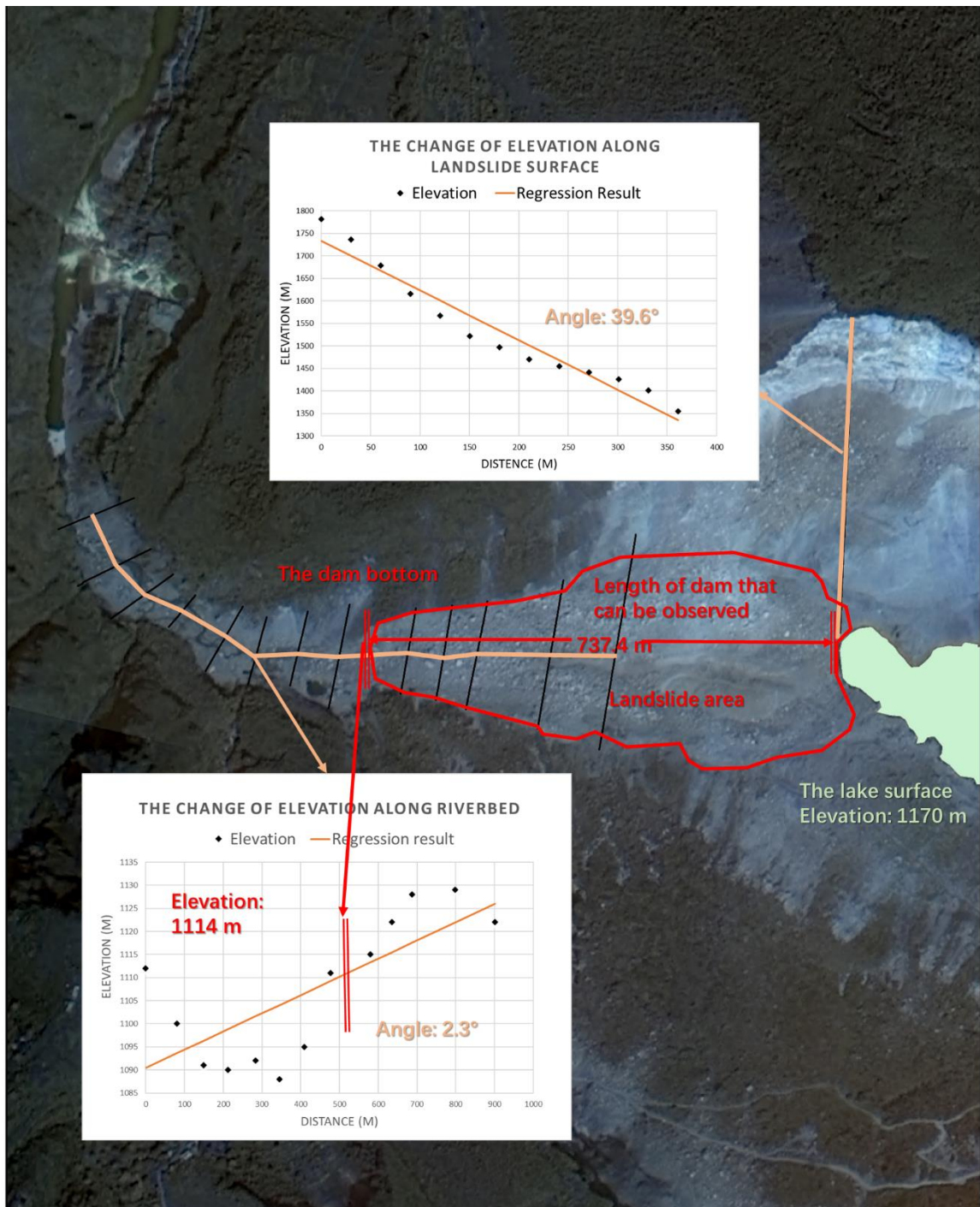
Another case for validation is Hongshiyuan landslide dam, a landslide created by moderate earthquake (Ms 6.5) on August 3<sup>rd</sup>, 2014. The epicenter of the earthquake is located at 27.11° N, 103.35° E and the landslide is 8.8 km southeast from the epicenter(Luo et al., 2019). The landslide dam is over 78 meters above the water, holding a maximum water storage of  $2.6 \times 10^8 \text{ m}^3$ (Zhou et al., 2015). Breaching of this giant dam will not only pose a high threat to the residents who live around, but also bring a possibility to damage other hydropower dams downstream. The data used to carry out the procedure in this research and predict the essential geometry parameter of landslide dam is listed in Table 1, including an after-landslide remote sensing image(2 m solution) and a pre-event DEM.

<u>Input data</u>	<u>Source</u>	<u>Description</u>
<u>After-landslide Remote sensing image</u>	<u>Gaofen-1 satellite</u>	<u>2 m solution</u>
<u>Pre-landslide DEM</u>	<u>SRTM V3</u>	<u>30 m solution</u>
<u>Repose angle of the debris</u>	<u>Relative case recording</u>	<u>Rough estimation</u>
<u>The elevation of riverbed</u>	<u>Sampling from DEM</u>	<u>Rough estimation</u>

Table 1 Source of input data used in the Hongshiyuan case.

Firstly, the image and the DEM is used to obtain the parameters required to make the prediction. The elevation of the lake level is obtained by sampling lake edge points. As shown in Fig 10, the elevation of the water level on the place of dam bottom before the landslide can be obtained through sampling the lowest points along the riverbed in the DEM (every lowest point in each black line), which is 1114m. The lake level is 1170 m. As the water depth of Niulan River is about 3 m(Zhou et al., 2015), the elevation of the dam bottom is 1111m. Therefore, the difference between them,  $H_m$ , is 59 m. The length of the landslide dam that can be observed,  $L_m$ , is measured directly in the image, which is 737.4 m (Fig 10).

335



336

337

Fig 10 Hongshiyuan landslide dam (image from Gaofen -1 satellite)

338

As shown in the Fig 10, we can acquire the angle of the riverbed  $\theta$  and the landslide surface  $\alpha$  through analysis of the change of the elevation along the river and the landslide track. As the recording of the repose angle of the debris is missing, the average value of other cases is taken as a rough estimation.

339

340

And the recording of repose angle  $\varphi$  is missing, it is set as 35.5°, according to the average value of other landslide dam(Wang et al., 2013).

341

342

Putting the parameters above into the model proposed in 3.3, we can calculate the highest elevation of the dam crest. As it is the lowest elevation of the dam crest that decides the break of dam, formula (9) is

344

used to fitting the relationship between the lowest crest and the highest crest. The elevation of the lowest elevation of the dam crest is 1123.7 m. And the potential maximum volume of the lake can be calculated easily with the DEM. The comparison of field survey and predicting outcome is shown in Table 2, which suggests a strong consistency between them.(Zhou et al., 2015; Luo et al., 2019)

<u>Parameter</u>	<u>Measured data</u>	<u>The predicting outcome</u>	<u>Error</u>
<u>the lowest elevation of the dam top</u>	<u>1222(m)</u>	<u>1223.7(m)</u>	<u>1.7(m)</u>
<u>the maximum of lake volume</u>	<u><math>2.6 \times 10^8 (m^3)^*</math></u>	<u><math>3.1 \times 10^8 (m^3)</math></u>	<u><math>0.4 \times 10^8 (m^3)^*</math></u>

Table 2 predicting outcome and measured data from field survey(Zhou et al., 2015; Luo et al., 2019).

## 5. Discussion

### 5.1. ~~Rapid hazard assessment~~Rapid hazard assessment

The lowest height of the dam crest and the maximum volume of the barrier lake are important input parameters for the dam-breaking model-. This paper has given the procedure to obtain them rapidly. We take Baige landslide dam as an example to illustrate how to use the prediction results to carry out rapidly hazard assessment.

Many scholars have found the correlation between the geometric parameters of landslide dam and its risk by empirical formula. On the basis of the prediction results and the formulas they provide, we can make a quick prediction of the key information of the landslide dam hazard, such as the dam volume, the stability of the barrier dam and the potential maximum discharge of the lake.

The width of the barrier dam can be obtained directly from remote sensing images, which is 574.6m.

As the edge and Angle conditions in the simplified model (Fig 4) have been cleared, that is, all the simplified section plane parameters in the model can be obtained. So based on the relationship between edges and angles in the model, the distance between top and bottom in the lowest crest,  $H'_t$ , and the

length of the dam top,  $L'_T$ , can be expressed by the following formula (10), (11).

$$H'_t = \cos \theta (0.63 H_h + 5.59 - H_r) \quad (10)$$

$$L'_T = L'_B - \frac{H'}{\tan \beta_d} - \frac{H'}{\tan \beta_u} \quad (11)$$

However, because the cross section of the barrier dam is not evenly distributed in the direction of the

370 vertical river, the height change will occur as discussed in 3.5. We can assume that the change of its top  
 371 height is basically linear and the bottom side length and top side length of the section trapezoid do not  
 372 change in the direction of the vertical channel. Therefore, we can obtain the estimation Formula (12) to  
 373 calculate the volume of the dam debris. In the case of Baige landslide dam, the prediction outcome is  
 374  $32.4 \times 10^6 m^3$ , and the true value according to field survey is  $30.2 \times 10^6 m^3$  (Shen et al., 2020). The  
 375 error is mainly induced by the elevation change of riverbed in the direction of the vertical channel., which  
 376 has a great influence to area of the dam section when the width of the dam is large.

377 
$$V_d = \frac{1}{4} W (H'_l + H'_r) (L'_B + L'_T) \quad (12)$$

378 In Dong research, a regression model to evaluate the stability of the barrier lake is proposed based on the  
 379 case of the historical landslide dam (Dong et al., 2011a), as shown in Formula (13).

380 
$$L_s = -2.55 \log(P) - 3.64 \log(H_l) + 2.99 \log(W) + 2.73(L) - 3.87 \quad (13)$$

381 Where  $P, H_l, W, L$  are the inflow, dam height, width and length of the landslide dam. In the case of  
 382 Baige landslide, the inflow of Baige landslide dam is  $822 m^3 / s$  (Li et al., 2019). The result  $L_s$  is -  
 383 1.472, which means that Baige landslide dam is unstable and has a high risk to breach.

384 -In the simple prediction formula (149) proposed by Cenderelli., V is the maximum volume of the  
 385 dammed lake, and Q is the maximum flood peak of dam breaching. Without treatment, the largest flood  
 386 peak of the Baige Landslide Dam breaching will reach  $42257 (m^3 / s)$ .

387

388 
$$Q = 3.4 \cdot V^{0.46} \quad (149)$$

389

390 The comparison between the predicted result and the measured date, as shown in table 34, achieves a  
 391 good agreement. The rapid assessment of the dam breaching hazard has been completed. As the  
 392 simulation model of dam breaching has a significant influence on the prediction of these factors~~these factors~~  
 393 peak, they should also be selected carefully in practical applications. Besides Cenderelli's formulas ~~above~~,  
 394 there are also many other formulas to choose to complete the prediction~~predict the dam breaching~~ (Costa  
 395 and Schuster, 1991; Walder and OConnor, 1997; Shi et al., 2014; Ruan et al., 2021; Peng and Zhang,  
 396 2012; Zhong et al., 2018; Ermini and Casagli, 2003; Dong et al., 2011a; Shen et al., 2020). And many  
 397 scholars have discussed the merits and demerits between these hazard assessment models (Peng and  
 398 Zhang, 2012; Fan et al., 2021).

399

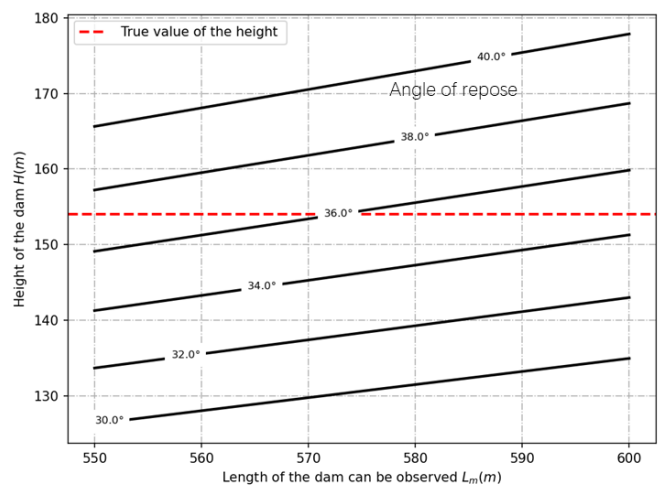
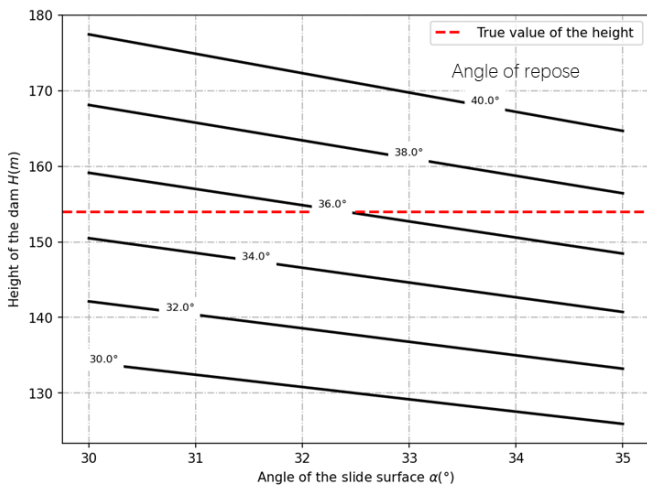
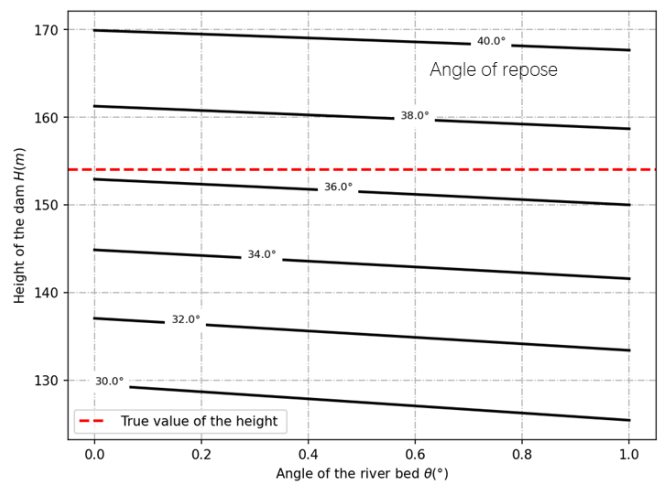
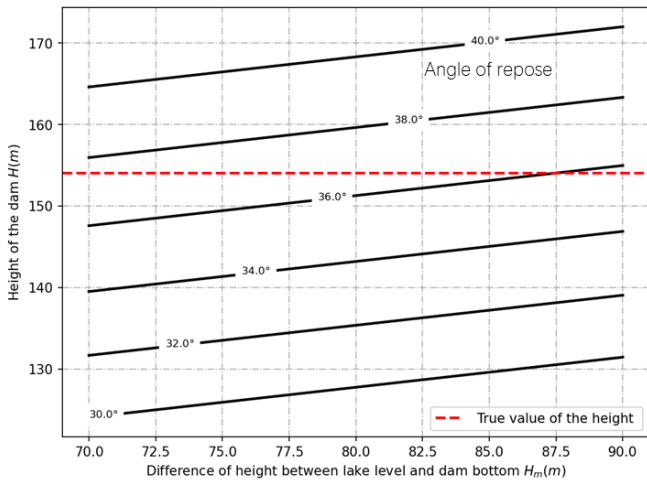
Parameter	Measured data	The <del>present-</del> <u>method predicting</u> <u>outcome</u>
<u>T</u> the highest elevation of the dam top	3014 (m)	3016.5(m)

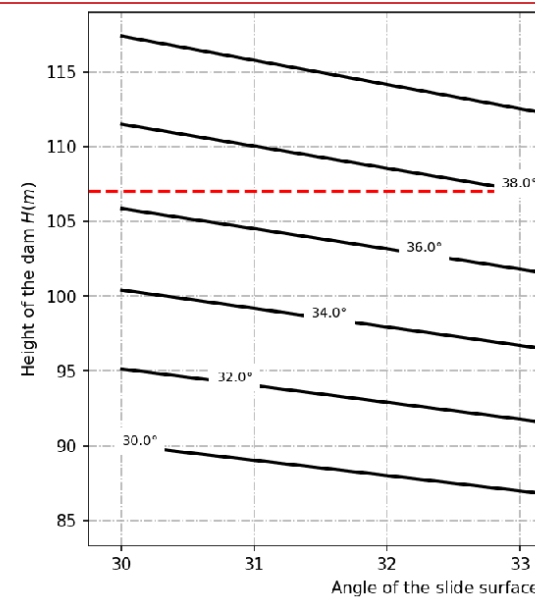
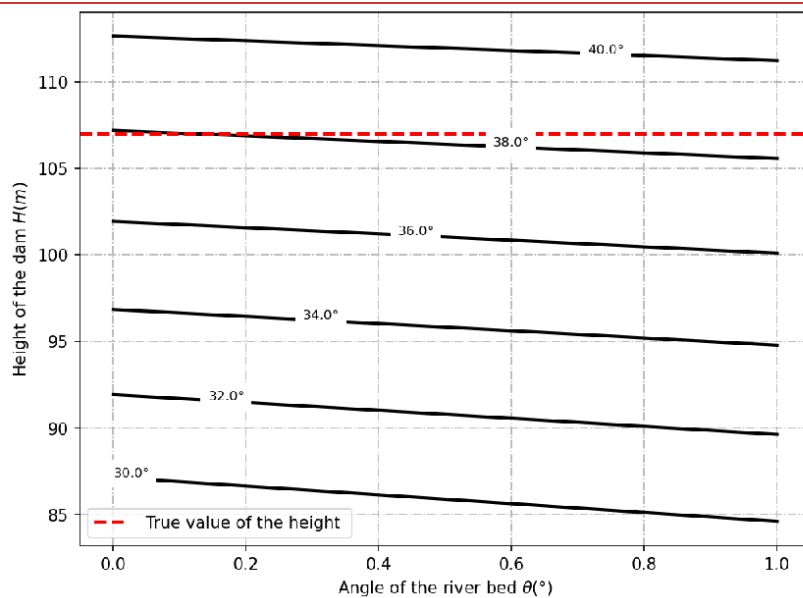
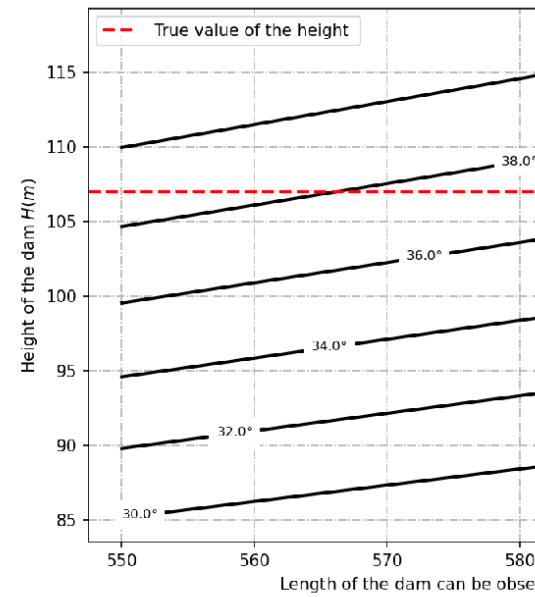
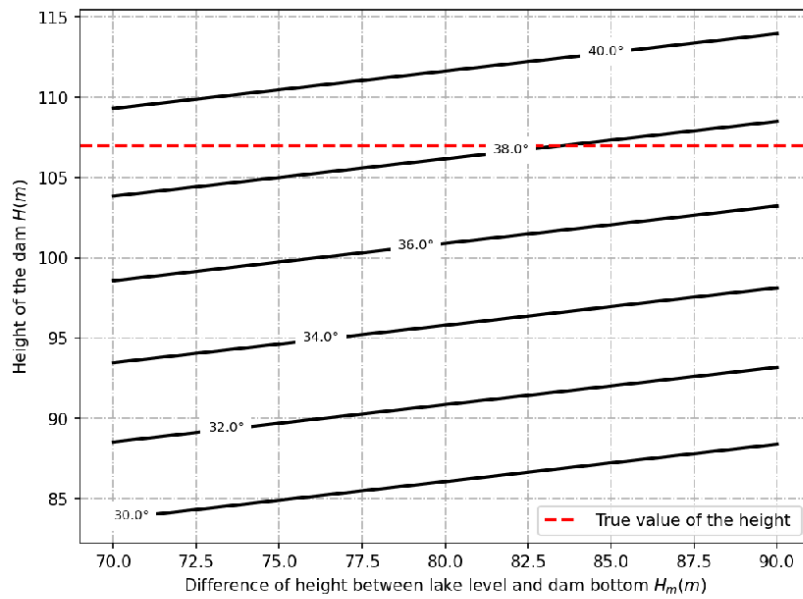
The lowest elevation of the dam top	2967 (m)	2964.2(m)
The maximum of lake volume	$8.69 \times 10^8 (m^3)^*$	$7.96 \times 10^8 (m^3)$
<u>The dam volume</u>	<u><math>30.2 \times 10^6 (m^3)</math></u>	<u><math>32.4 \times 10^6 (m^3)</math></u>
<u>The stability of dam</u>	<u>Not stable</u>	<u>Not stable</u>
<u>The peak discharge</u>	<del><math>41624 (m^3 / s)^*</math></del>	$42257 (m^3 / s)$
	<u><math>41624 (m^3 / s)^*</math></u>	

Table 3+ the comparison of the measured data and the predicted result. As relative measures have been taken to reduce the maximum volume of the barrier lake, data with star in the table is the estimation results of Chen's detailed back analyses(Chen et al., 2020).

## 5.2. Sensitivity analysis

In this procedure, the main parameters include: the length of the dam that can be observed, the elevation of the lake level, the elevation of the dam bottom, the slope angle of landslide surface and the inclination angle of the riverbed. Since  $H_m$  is the lake level elevation minus the elevation of the dam bottom, sensitivity analysis of these two parameters will be conducted on  $H_m$  directly. The variation of the prediction result with the change of parameters is shown as follows:





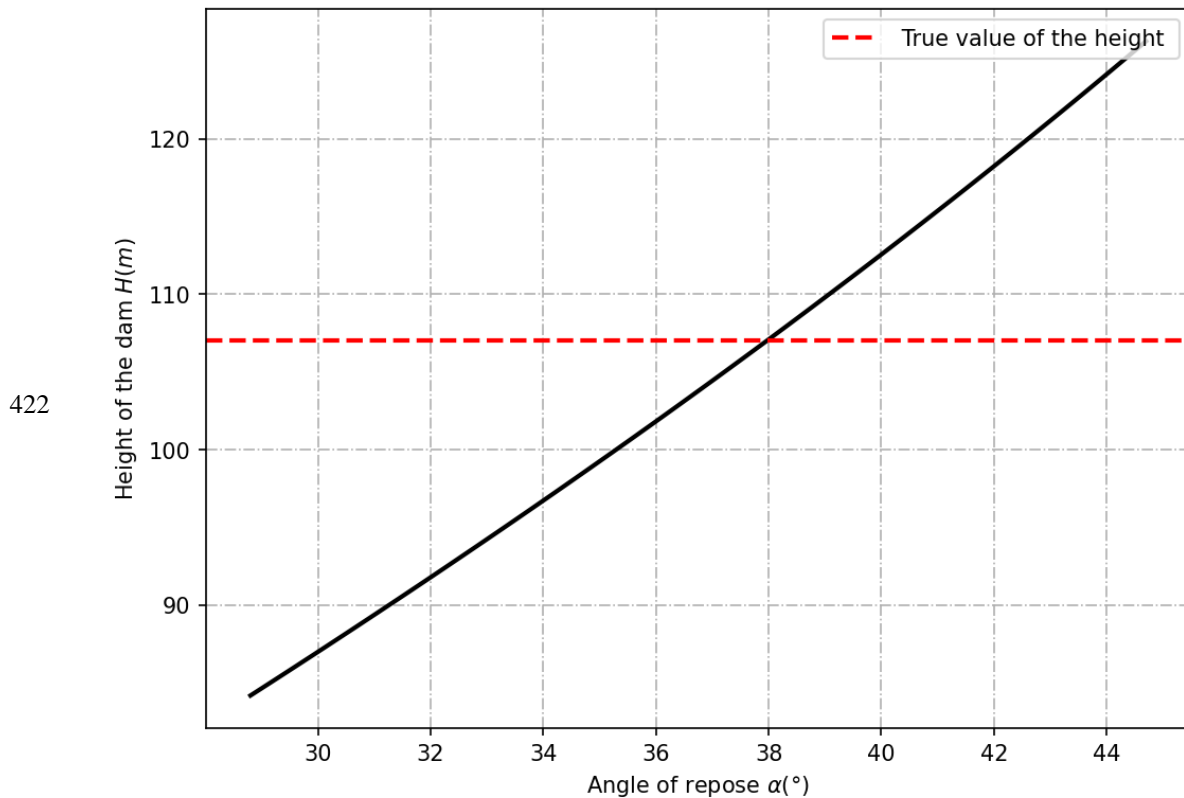
410

411 Fig 119 the relationship between the predicted result and the input parameters.

412

413 As can be seen from Fig 119, with other parameters unchanged, the greater the observable length of the  
 414 dam and the difference of height between the lake level and dam bottom, the higher the dam crest. The  
 415 crest of the dam gets lower as the slope angle of landslide surface and the inclination angle of the riverbed  
 416 rise. The slope foot of the dam is mainly affected by the angle of landslide surface and inclination angle  
 417 of the riverbed. The smaller the slope foot, the smaller the height of the dam. The calculated results are  
 418 in good agreement with expectations.

419 Meantime, it can be found that these parameters all have an impact of about 10% on the final prediction  
 420 results. So, it is necessary to be careful to determine these parameters. Possible methods to reduce errors  
 421 include repeat procedures and more reliable historical data.



423 Fig 129 the relationship between the predicted result and the angle of repose.

424

425 Finally, it is found that the angle of repose of the dam body has a significant influence on the height of  
 426 the dam (Fig 129). The greater the angle of repose, the greater the estimate of dam height. According to  
 427 Wang's field survey, the angle of repose of the landslide dams in Wenchuan earthquake ranges from 28.8°  
 428 to 44.7°, with an average value of 35.5°(Wang et al., 2013). In the absence of the historical date, the  
 429 average value proposed by Wang can be used. However, in this way, the difference between the final  
 430 result and the true value can be about 30% in the worst case. Therefore, on the premise of sufficient  
 431 disaster relief resources, it is better to make a bad estimate of the repose angle, so as not to make a wrong  
 432 judgment on the hazard. On the other hand, it is also possible to check the repose angle of the material  
 433 in advance in landslide prone area, so as to make a quick hazard assessment after the landslide.

### 434 5.3. Influence of image solution

435 The remote sensing image used in this research is Beijing-1 with a resolution of 0.8m. The pre-landslide  
 436 DEM is SRTM V3 with a resolution of 30m. As more and more remote sensing data are available, in  
 437 addition to satellite-based remote sensing platform, small UAV remote sensing platform can also be well  
 438 applied to this procedure. As different sensors and remote sensing platforms may have different  
 439 resolutions, we use interpolation to obtain images with different resolutions to explore the appropriate  
 440 resolution for this procedure (Table 2; Table 3).

441



Resolution	Input						
	$H_1$ (m)	$H_0$ (m)	$H_m$ (m)	$L_m$ (m)	$\alpha$ (°)	$\theta$ (°)	$\varphi$ (°)
0.8	2944	2860	84	567	30.65	0.11	35.5
5	2946	2861	70	545	28.58	0.10	35.5
15	2943	2856	73	562	29.44	0.09	35.5
30	2956	2862	84	540	29.10	0.16	35.5

442 Table 42 the parameters obtained through different resolution image, where  $H_1$  is the elevation of the  
443 lake level,  $H_0$  is the elevation of the dam bottom,  $H_m$  is  $H_1$  minus  $H_0$ ,  $L_m$  is the length of the  
444 dam that can be observed in the image,  $\alpha$  is the slope angle of landslide surface,  $\theta$  is the inclination  
445 angle of the riverbed and  $\varphi$  is the angle of repose

Resolution	Output		Accuracy	
	$H$ (m)	True value $H$ (m)	Error(m)	
0.8	2964.2	2967	2.8	
5	2964.7	2967	2.3	
15	2961.6	2967	5.4	
30	2960.5	2967	6.5	

446 Table 53 the predicted result of image with different resolutions  
447 As we discussed before, the main parameters in this procedure include the length of the dam that can be  
448 observed, the lake level, the elevation of the dam bottom, the slope angle of landslide surface and the  
449 inclination angle of the riverbed. Obviously, the resolution of the image will affect all of these five (Table  
450 42), but mainly affect the determining of length of the dam that can be observed and the lake level. In  
451 general, the higher the resolution, the more accurate the prediction results obtained. When the resolution  
452 drops from 0.8m to 30m, the error of prediction results changes from 2.8m to 6.5m, as shown in Table  
453 53. But for the procedure this paper proposed, image with resolution of 5m is sufficient for a good  
454 estimate of the dam height.

455 There is no doubt that the resolution and quality of DEM data are very important for this procedure.  
456 However, due to the lack of comparative data, this paper does not conduct in-depth discussion on it. For  
457 this part, Dong has had relevant discussions in his research(Dong et al., 2014) for readers' reference.

## 458 5.4. Other discussion

459 In this study, the ~~predicting model of is mainly based on the formation mechanism of the barrier dam was~~  
460 ~~mainly based on Wu's experiment, combined dam combined~~ with a single remote sensing image and pre-  
461 landslide DEM to quickly predict the essential paraments of the landslide dam hazard. Therefore, a more  
462 comprehensive assessment of the reliability of ~~formation mechanism Wu's theory~~ has also been carried  
463 out. It is found that most laws can be applied well, but formula (3) has greater limitations in fitting the  
464 "cut-top" effect. In Wu's experiment, the "cut-top" effect fitting is mainly determined by the slope angle  
465 of landslide surface. Actually, the angle between the riverbed plane and slop surface of the dam should

466 be determined by its landslide potential energy, landslide length, and landslide angle(Grasselli et al., 2000;  
467 Xu et al., 2013; Iverson et al., 2015). In addition to the slope angle of landslide surface, the length of the  
468 landslide and potential energy are equally important. In Wu's formula, only the slope angle of landslide  
469 surface is considered, so more experiments are needed to improve the fitting.

470 As there is not enough theoretical research to support the prediction of the lowest elevation of the dam  
471 crest, the method proposed in this paper still has certain limitations. In addition, the mechanism of the  
472 relationship between the highest elevation of the dam crest and the lowest elevation of the dam crest is  
473 not clear. In most cases, when it comes to the height of a barrier lake, usually only the highest or lowest  
474 elevation is recorded, resulting in fewer complete records of both parameters. As the recording in most  
475 cases is not completed, only a small number of cases are used to carry out the fitting. Therefore, this  
476 aspect still needs more work and related research to support relevant predictions.

477

## 478 6. Conclusion

479 This research proposes a procedure based on a single remote sensing image to predict the height of the  
480 dam crest and rapidly assess the hazard. With the after-landslide remote sensing image, it only takes no  
481 more than one human hour to complete the whole procedure. Compared with Dong's procedure([Dong  
482 et al., 2014](#)), this method only requires only one single remote sensing image and has a wider applicability.  
483 In view of the large topographic changes in the landslide area, a more reasonable method of using the  
484 pre-landslide DEM is proposed. Even the use of poor-quality DEM can complete the relevant prediction  
485 and hazard assessment. In the case of Baige Landslide Dam, by extracting the barrier lake surface  
486 elevation and determining the bottom elevation of the dam, the prediction of the highest elevation of the  
487 dam crest is completed, and the difference between the predicted results and the measured data is within  
488 3m. Since the lowest point of the dam crest determines the potential maximum volume of the barrier lake,  
489 we based on historical records find that the height of the highest point and the lowest point of the landslide  
490 dam crest basically conforms to the linear relationship. The relationship is expressed as a formula ([98](#))  
491 through unary fitting. The prediction result of the lowest elevation of the top of the Baige Landslide Dam  
492 is 2964.2m, whose error is 2.8m compared to data from field survey, 2967 m. which is consistent with  
493 the field measurement results, 2967m. And in the case of Hongshiyan landslide dam, the error of  
494 predicting result of dam top elevation is 1.7m. Based on the empirical formula, the potential maximum  
495 flood peak of the dam break without treatment is predicted, which is basically consistent with the  
496 prediction of a more sophisticated model(Zhang et al., 2019; Chen et al., 2020, 2021; Tian et al., 2020).

497

498 In the discussion part, some essential parameters of landslide dam, such as the volume of the dam, the  
499 stability of the dam and the potential maximum flood peak of the dam break without treatment, is  
500 calculated based on the predicting result, which is basically consistent with the true value. —T  
501 the sensitivity of the parameters used in this method is analyzed, and it is found that the repose angle of the

502 landslide material can affect the prediction result up to 30%. Therefore, the repose angle should be  
503 carefully determined when using this procedure for related applications. Finally, through experiment with  
504 different resolutions of remote sensing images, we find that as the resolution becomes lower, the accuracy  
505 of this method decreases. The resolution of 5m and above is a reasonable range for applying this method,  
506 otherwise it will be difficult to distinguish the dam body and the water boundary.

## 507 **Data availability**

508 The data are available from the authors upon request.

## 509 **Author Contributions**

510 WJZ designed the experiments, and YZ carried them out. SXW and FTW gave some very important  
511 suggestions on basic knowledge of landslide dams. LTW, WLL, ZQ and JFZ helped to operate the whole  
512 procedure. QG, ZQW helped with some figures, and YBX provided some remote sensing images. FTW  
513 prepared the manuscript with contributions from all co-authors.

## 514 **Competing interests**

515 The authors declare that they have no conflict of interest.

## 516 **Acknowledgements**

517 We appreciate the constructive reviews provided by three anonymous reviewers and editor Hans-Balder  
518 Havenith. The authors acknowledge the support from the National Key R&D Program of China under  
519 Grant 2017YFB0504101 and Grant 2021YFB3901201.

## 520 **Financial support**

521 This research has been supported by the National Key R&D Program of China under Grant  
522 2017YFB0504101 and Grant 2021YFB3901201.

523

524

525

## 526 **Reference**

527 Adams, J.: Earthquake-dammed lakes in New Zealand, 9, 215–219, 1981.

528 Anon: Exploring machine learning potential for climate change risk assessment, 103752,  
529 <https://doi.org/10.1016/j.earscirev.2021.103752>, 2021.

530 Ayalew, L. and Yamagishi, H.: The application of GIS-based logistic regression for landslide  
531 susceptibility mapping in the Kakuda-Yahiko Mountains, Central Japan, *Geomorphology*, 65, 15–31,  
532 <https://doi.org/10.1016/j.geomorph.2004.06.010>, 2005.

533 Braun, A., Cuomo, S., Petrosino, S., Wang, X., and Zhang, L.: Numerical SPH analysis of debris flow  
534 run-out and related river damming scenarios for a local case study in SW China, *Landslides*, 15, 535–  
535 550, <https://doi.org/10.1007/s10346-017-0885-9>, 2018.

536 Briaud, J.-L.: Case Histories in Soil and Rock Erosion: Woodrow Wilson Bridge, Brazos River Meander,  
537 Normandy Cliffs, and New Orleans Levees, 134, 1425–1447, [https://doi.org/10.1061/\(ASCE\)1090-0241\(2008\)134:10\(1425\)](https://doi.org/10.1061/(ASCE)1090-0241(2008)134:10(1425)), 2008.

539 Canuti, P., Casagli, N., Ermini, L., Fanti, R., and Farina, P.: Landslide activity as a geoinicator in Italy:  
540 significance and new perspectives from remote sensing, *Environ. Geol.*, 45, 907–919,  
541 <https://doi.org/10.1007/s00254-003-0952-5>, 2004.

542 Cao, Z., Yue, Z., and Pender, G.: Landslide dam failure and flood hydraulics. Part II: coupled  
543 mathematical modelling, 59, p.1021-1045, 2011.

544 Chen, C.-Y., Chen, T.-C., Yu, F.-C., and Hung, F.-Y.: A landslide dam breach induced debris flow – a case  
545 study on downstream hazard areas delineation, *Env Geol*, 47, 91–101, <https://doi.org/10.1007/s00254-004-1137-6>, 2004.

547 Chen, X. and Lu: Geomatics-based Method Research on Capacity Calculation of Quake Lake, 2008.

548 Chen, Z., Chen, S., and Wang, L.: Back analysis of the breach flood of the 11.03 Baige barrier lake at the  
549 Upper Jinsha River, 2020.

550 Chen, Z., Zhou, H., Ye, F., Liu, B., and Fu, W.: The characteristics, induced factors, and formation  
551 mechanism of the 2018 Baige landslide in Jinsha River, Southwest China, *Catena*, 203, 105337,  
552 <https://doi.org/10.1016/j.catena.2021.105337>, 2021.

- 553 Costa, J. E. and Schuster, R. L.: The formation and failure of natural dams, 100, 1054–1068,  
554 [https://doi.org/10.1130/0016-7606\(1988\)100<1054:TFAFON>2.3.CO;2](https://doi.org/10.1130/0016-7606(1988)100<1054:TFAFON>2.3.CO;2), 1988.
- 555 Costa, J. E. and Schuster, R. L.: Documented historical landslide dams from around the world,  
556 Documented historical landslide dams from around the world, U.S. Geological Survey, Vancouver, WA,  
557 <https://doi.org/10.3133/ofr91239>, 1991.
- 558 Cui, P., Zhu, Y., Han, Y., Chen, X., and Zhuang, J.: The 12 May Wenchuan earthquake-induced landslide  
559 lakes: distribution and preliminary risk evaluation, *Landslides*, 6, 209–223,  
560 <https://doi.org/10.1007/s10346-009-0160-9>, 2009.
- 561 Dong, J.-J., Tung, Y.-H., Chen, C.-C., Liao, J.-J., and Pan, Y.-W.: Logistic regression model for predicting  
562 the failure probability of a landslide dam, *Engineering Geology*, 117, 52–61,  
563 <https://doi.org/10.1016/j.enggeo.2010.10.004>, 2011a.
- 564 Dong, J.-J., Tung, Y.-H., Chen, C.-C., Liao, J.-J., and Pan, Y.-W.: Logistic regression model for predicting  
565 the failure probability of a landslide dam, *Engineering Geology*, 117, 52–61,  
566 <https://doi.org/10.1016/j.enggeo.2010.10.004>, 2011b.
- 567 Dong, J.-J., Lai, P.-J., Chang, C.-P., Yang, S.-H., Yeh, K.-C., Liao, J.-J., and Pan, Y.-W.: Deriving  
568 landslide dam geometry from remote sensing images for the rapid assessment of critical parameters  
569 related to dam-breach hazards, *Landslides*, 11, 93–105, <https://doi.org/10.1007/s10346-012-0375-z>,  
570 2014.
- 571 Ermini, L. and Casagli, N.: Prediction of the behaviour of landslide dams using a geomorphological  
572 dimensionless index, 28, 31–47, <https://doi.org/10.1002/esp.424>, 2003.
- 573 Fan, X., van Westen, C. J., Xu, Q., Gorum, T., and Dai, F.: Analysis of landslide dams induced by the  
574 2008 Wenchuan earthquake, *Journal of Asian Earth Sciences*, 57, 25–37,  
575 <https://doi.org/10.1016/j.jseaes.2012.06.002>, 2012.
- 576 Fan, X., Dufresne, A., Siva Subramanian, S., Strom, A., Hermanns, R., Tacconi Stefanelli, C., Hewitt, K.,  
577 Yunus, A. P., Dunning, S., Capra, L., Geertsema, M., Miller, B., Casagli, N., Jansen, J. D., and Xu, Q.:  
578 The formation and impact of landslide dams – State of the art, *Earth-Science Reviews*, 203, 103116,  
579 <https://doi.org/10.1016/j.earscirev.2020.103116>, 2020.
- 580 Fan, X., Dufresne, A., and Whiteley, J.: Recent technological and methodological advances for the  
581 investigation of landslide dams, 218, 103646, <https://doi.org/10.1016/j.earscirev.2021.103646>, 2021.
- 582 Grasselli, Y., Herrmann, H. J., Oron, G., and Zapperi, S.: Effect of impact energy on the shape of granular  
583 heaps, *GM*, 2, 97–100, <https://doi.org/10.1007/s100350050039>, 2000.
- 584 Han, Y., Chun, Q., and Wang, H.: Quantitative safety evaluation of ancient Chinese timber arch lounge  
585 bridges, *Journal of Wood Science*, 68, 4, <https://doi.org/10.1186/s10086-022-02011-y>, 2022.
- 586 Iverson, R. M., George, D. L., Allstadt, K., Reid, M. E., Collins, B. D., Vallance, J. W., Schilling, S. P.,  
587 Godt, J. W., Cannon, C. M., and Magirl, C. S.: Landslide mobility and hazards: implications of the 2014  
588 Oso disaster, 2015.
- 589 Li, H., Qi, S., Chen, H., Liao, H., Cui, Y., and Zhou, J.: Mass movement and formation process analysis  
590 of the two sequential landslide dam events in Jinsha River, Southwest China, *Landslides*, 16, 2247–2258,  
591 <https://doi.org/10.1007/s10346-019-01254-z>, 2019.
- 592 Li, T. C., Schuster, R. L., and Wu, J. S.: Landslide dams in south-central China, 1986.
- 593 Luo, J., Pei, X., Evans, S. G., and Huang, R.: Mechanics of the earthquake-induced Hongshiyuan landslide  
594 in the 2014 Mw 6.2 Ludian earthquake, Yunnan, China, *Engineering Geology*, 251, 197–213,  
595 <https://doi.org/10.1016/j.enggeo.2018.11.011>, 2019.

- 596 Meng, C.-K., Chen, K.-T., Niu, Z.-P., Di, B.-F., and Ye, Y.-J.: Influence of Internal Structure on Breaking  
597 Process of Short-Lived Landslide Dams, 9, 2021.
- 598 Mora Castro, S.: The 1992 Río Toro landslide dam, Costa Rica, *Landslide News*, 1993.
- 599 Morgenstern, R., Massey, C., Rosser, B., and Archibald, G.: Landslide Dam Hazards: Assessing Their  
600 Formation, Failure Modes, Longevity and Downstream Impacts, 2021.
- 601 Peng, M. and Zhang, L. M.: Breaching parameters of landslide dams, *Landslides*, 9, 13–31,  
602 <https://doi.org/10.1007/s10346-011-0271-y>, 2012.
- 603 Ruan, H., Chen, H., Wang, T., Chen, J., and Li, H.: Modeling Flood Peak Discharge Caused by  
604 Overtopping Failure of a Landslide Dam, 13, 921, <https://doi.org/10.3390/w13070921>, 2021.
- 605 Shen, D., Shi, Z., Peng, M., Zhang, L., and Jiang, M.: Longevity analysis of landslide dams, 17, 2020.
- 606 Shi, Z., Ma, X., and Peng, M.: STATISTICAL ANALYSIS AND EFFICIENT DAM BURST  
607 MODELLING OF LANDSLIDE DAMS BASED ON A LARGE-SCALE DATABASE, 33, 1780–1790,  
608 2014.
- 609 Walder, J. S. and OConnor, J. E.: Methods for predicting peak discharge of floods caused by failure of  
610 natural and constructed earthen dams, *Water Resour. Res.*, 33, 2337–2348,  
611 <https://doi.org/10.1029/97WR01616>, 1997.
- 612 Wang, J.-J., Zhao, D., Liang, Y., and Wen, H.-B.: Angle of repose of landslide debris deposits induced  
613 by 2008 Sichuan Earthquake, *Eng. Geol.*, 156, 103–110, <https://doi.org/10.1016/j.enggeo.2013.01.021>,  
614 2013.
- 615 Wang, Z. H. and Lu, J. T.: Satellite monitoring of the Yigong landslide in Tibet, China, in: *Earth  
616 Observing Systems VII*, Bellingham, 34–38, <https://doi.org/10.1117/12.453739>, 2002.
- 617 Wu, H., Nian, T., Chen, G., Zhao, W., and Li, D.: Laboratory-scale investigation of the 3-D geometry of  
618 landslide dams in a U-shaped valley, *Engineering Geology*, 265, 105428,  
619 <https://doi.org/10.1016/j.enggeo.2019.105428>, 2020.
- 620 Xu, W.-J., Xu, Q., and Wang, Y.-J.: The mechanism of high-speed motion and damming of the  
621 Tangjiashan landslide, *Eng. Geol.*, 157, 8–20, <https://doi.org/10.1016/j.enggeo.2013.01.020>, 2013.
- 622 Yang, S.-H., Pan, Y.-W., Dong, J.-J., Yeh, K.-C., and Liao, J.-J.: A systematic approach for the assessment  
623 of flooding hazard and risk associated with a landslide dam, *Nat Hazards*, 65, 41–62,  
624 <https://doi.org/10.1007/s11069-012-0344-9>, 2013.
- 625 Yunjian, G., Siyuan, Z., Jianhui, D., Zhiqiu, Y., and Mahfuzur, R.: Flood assessment and early warning  
626 of the reoccurrence of river blockage at the Baige landslide, *J. Geogr. Sci.*, 31, 1694–1712,  
627 <https://doi.org/10.1007/s11442-021-1918-9>, 2021.
- 628 Zhang, L., Xiao, T., He, J., and Chen, C.: Erosion-based analysis of breaching of Baige landslide dams  
629 on the Jinsha River, China, in 2018, 2019.
- 630 Zhong, Q. M., Chen, S. S., Mei, S. A., and Cao, W.: Numerical simulation of landslide dam breaching  
631 due to overtopping, *Landslides*, 15, 1183–1192, <https://doi.org/10.1007/s10346-017-0935-3>, 2018.
- 632 Zhou, J., Cui, P., and Hao, M.: Comprehensive analyses of the initiation and entrainment processes of  
633 the 2000 Yigong catastrophic landslide in Tibet, China, *Landslides*, 13, 39–54,  
634 <https://doi.org/10.1007/s10346-014-0553-2>, 2016.
- 635 Zhou, X., Chen, Z., Yu, S., Wang, L., Deng, G., Sha, P., and Li, S.: Risk analysis and emergency actions  
636 for Hongshiyuan barrier lake, *Nat Hazards*, 79, 1933–1959, <https://doi.org/10.1007/s11069-015-1940-2>,  
637 2015.

